βL–βM loop in the C-terminal domain of G protein-activated inwardly rectifying K$^+$ channels is important for G$_{\beta\gamma}$ subunit activation

Melissa Finley, Christine Arrabit, Catherine Fowler, Ka Fai Suen and Paul A. Slesinger

The Salk Institute for Biological Studies, La Jolla, CA 92037, USA

The activity of G protein-activated inwardly rectifying K$^+$ channels (GIRK or Kir3) is important for regulating membrane excitability in neuronal, cardiac and endocrine cells. Although G$_{\beta\gamma}$ subunits are known to bind the N- and C-termini of GIRK channels, the mechanism underlying G$_{\beta\gamma}$ activation of GIRK is not well understood. Here, we used chimeras and point mutants constructed from GIRK2 and IRK1, a G protein-insensitive inward rectifier, to determine the region within GIRK2 important for G$_{\beta\gamma}$ binding and activation. An analysis of mutant channels expressed in *Xenopus* oocytes revealed two amino acid substitutions in the C-terminal domain of GIRK2, GIRK2$_{L344E}$ and GIRK2$_{G347H}$, that exhibited decreased carbachol-activated currents but significantly enhanced basal currents with coexpression of G$_{\beta\gamma}$ subunits. Combining the two mutations (GIRK2$_{EH}$) led to a more severe reduction in carbachol-activated and G$_{\beta\gamma}$-stimulated currents. Ethanol-activated currents were normal, however, suggesting that G protein-independent gating was unaffected by the mutations. Both GIRK2$_{L344E}$ and GIRK2$_{EH}$ also showed reduced carbachol activation and normal ethanol activation when expressed in HEK-293T cells. Using epitope-tagged channels expressed in HEK-293T cells, immunocytochemistry showed that G$_{\beta\gamma}$-impaired mutants were expressed on the plasma membrane, although to varying extents, and could not account completely for the reduced G$_{\beta\gamma}$ activation. *In vitro* G$_{\beta\gamma}$ binding assays revealed an ∼60% decrease in G$_{\beta\gamma}$ binding to the C-terminal domain of GIRK2$_{L344E}$ but no statistical change with GIRK2$_{EH}$ or GIRK2$_{G347H}$, though both mutants exhibited G$_{\beta\gamma}$-impaired activation. Together, these results suggest that L344, and to a lesser extent, G347 play an important functional role in G$_{\beta\gamma}$ activation of GIRK2 channels. Based on the 1.8 Å structure of GIRK1 cytoplasmic domains, L344 and G347 are positioned in the βL–βM loop, which is situated away from the pore and near the N-terminal domain. The results are discussed in terms of a model for activation in which G$_{\beta\gamma}$ alters the interaction between the βL–βM loop and the N-terminal domain.

(Received 29 September 2003; accepted after revision 05 January 2004; first published online 14 January 2004)

Corresponding author P. A. Slesinger: Peptide Biology Laboratory, The Salk Institute, 10010 N. Torrey Pines Road, La Jolla, CA 92037, USA. Email: slesinger@salk.edu

Many inhibitory neurotransmitters exert their actions by stimulating pertussis toxin (PTX)-sensitive G protein-coupled neurotransmitter receptors (GPCR), which in turn open G protein-activated inwardly rectifying K$^+$ channels (GIRK or Kir3) (Hille, 1992). K$^+$ ions exit the cell when GIRK channels open, thereby hyperpolarizing the cell's membrane potential and making it more difficult to elicit an action potential. The loss of GIRK channels leads to hyperexcitability and seizures in the brain (Signorini *et al.* 1997; Slesinger *et al.* 1997), cardiac abnormalities

(Wickman *et al.* 1998) and hyperactivity and reduced anxiety (Blednov *et al.* 2001). Four mammalian GIRK channel subunits (GIRK1–4) have been identified, which coassemble to form neuronal GIRK channels (Yamada *et al.* 1998). Coimmunoprecipitation studies using brain tissues have demonstrated that GIRK channels are composed of heteromultimers of GIRK1/2 and GIRK2/3 (Liao *et al.* 1996; Jelacic *et al.* 2000). In some areas of the brain, such as in the substantia nigra, GIRK channels may exist as GIRK2 homomultimers (Liao *et al.* 1996; Inanobe *et al.* 1999).

GIRK channels have the canonical features of the inwardly rectifying K$^+$ channel family (Kir1–7), which

---

includes cytoplasmic N- and C-terminal domains, two putative transmembrane domains (M1, M2), and a highly conserved pore–loop complex involved in ion selectivity (Doupnik *et al.* 1995). Of the seven distinct families of Kir channels, however, only GIRK channels are activated by G protein $G_{\beta\gamma}$ subunits (Logothetis *et al.* 1987; Reuveny *et al.* 1994; Wickman *et al.* 1994). In addition, GIRK channel activity is also regulated by G protein-independent signalling molecules. Intracellular Na^+, MgATP and PIP_2, and extracellular ethanol have all been reported to open GIRK channels in the absence of functional G proteins (Ho & Murrell-Lagnado, 1999; Kobayashi *et al.* 1999; Lewohl *et al.* 1999; Petit-Jacques *et al.* 1999; Zhang *et al.* 1999).

Since the discovery that $G_{\beta\gamma}$ subunits activate GIRK channels (Logothetis *et al.* 1987), the molecular mechanism through which $G_{\beta\gamma}$ subunits open the channel has remained elusive. Initially, studies using chimeras and biochemistry demonstrated that $G_{\beta\gamma}$ subunits bind directly to the N-terminal domain and the distal part of the C-terminal domain of GIRK1 (Huang *et al.* 1995; Inanobe *et al.* 1995; Kunkel & Peralta, 1995; Slesinger *et al.* 1995). Krapivinsky *et al.* (1998) examined the effects of synthetic peptides derived from GIRK1, GIRK4 or IRK1 on the biochemical binding of $G_{\beta\gamma}$ to GIRK1/4 channels and concluded that two regions within the C-terminal domain were important for $G_{\beta\gamma}$ binding and activation. He *et al.* (1999, 2002), on the other hand, examined the $G_{\beta\gamma}$ sensitivity of GIRK4 and IRK1 chimeras and identified specific amino acids in the N- and C-terminal domains that were important for generating either the agonist-activated or $G_{\beta\gamma}$-dependent basal current (He *et al.* 1999, 2002). At present, there is no clear consensus on which region of the GIRK channels is essential for $G_{\beta\gamma}$ activation.

To identify regions important for $G_{\beta\gamma}$ activation, we studied chimeras of GIRK2 and a G protein-insensitive inward rectifier (IRK1). We chose GIRK2 because GIRK2, unlike GIRK1, readily forms functional homomultimers in neurones as well as in heterologous expression systems (Slesinger *et al.* 1996; Inanobe *et al.* 1999) and because the identity of amino acids involved in $G_{\beta\gamma}$ activation of GIRK2 is unknown. The $G_{\beta\gamma}$ sensitivity of chimeras was evaluated in two different expression systems: *Xenopus* oocytes and mammalian cells. We also examined the response of each chimeric channel to ethanol, which served as an indicator of GIRK channel gating that is G protein independent (Kobayashi *et al.* 1999; Lewohl *et al.* 1999; Zhou *et al.* 2001). Finally, we measured the biochemical binding of $G_{\beta\gamma}$ to glutathione S-transferase (GST) fusion proteins containing the C-terminal domain of the different mutant channels. We identified two amino acids in the middle of the C-terminal domain of GIRK2 that contribute

to $G_{\beta\gamma}$ binding and activation. Some of these results have been published in the form of an abstract (Finley *et al.* 2003).

Methods

Molecular biology

GIRK1 was in pBSK (Kubo *et al.* 1993*b*), GIRK2a cDNA was in pBTG (Lesage *et al.* 1994) and IRK1 was in pBSK (Kubo *et al.* 1993*a*). Chimeras were constructed by identifying transition points between GIRK2 and IRK1, using CLUSTAL alignment analysis, as illustrated in Fig. 1*A*. The nomenclature, $I1G2_{xx-xx}$, refers to IRK1 (I1) and the amino acid sequence in GIRK2 ($G2_{xx-xx}$) in the chimeric channel. The following point mutations in GIRK2 were tested: F338Y, T343F, L344E, G347H, F348Y and L344E/G347H (EH). All mutants were constructed using PCR and the mutation confirmed with DNA sequencing. The following chimeras were constructed but did not lead to detectable currents when expressed in oocytes: $I1G2_{25-190}$, $I1G2_{25-414}$, $I1G2_{25-414}$, $I1G2_{51-414}$, $I1G2_{73-414}$, $I1G2_{97-271}$, $I1G2_{1-271}$, $I1G2_{97-310}$, $I1G2_{97-335}$ and $I1G2_{97-352}$.

In vitro methyl-capped cRNA was made from linear cDNA and T3 or T7 RNA polymerase (Stratagene). The quality of cRNA was estimated using an ethidium-stained formaldehyde gel and the concentration measured by UV spectrophotometry. *Xenopus* oocytes were isolated as previously described (Slesinger *et al.* 1996). Briefly, oocytes were surgically removed from one side of the frog under anaesthesia (0.1% tricaine), the frog was sutured, and then allowed to recover from surgery. The experimental procedures were approved by the Institutional Animal Care and Use Committee (IACUC) at The Salk Institute. Oocytes were injected with a 46 nl solution containing cRNA for the G protein $G_{\beta1}$ (∼2–8 ng) and $G_{\gamma2}$ (∼2–8 ng) subunits or the human muscarinic receptor (0.2–2 ng), and the GIRK channels (0.5–5 ng). In some experiments, βARK1-ct cRNA (∼6 ng) was coinjected with the cRNA for GIRK channels (He *et al.* 1999). Oocytes were incubated in ND96 (96 mM NaCl, 2 mM KCl, 1 mM $CaCl_2$, 1 mM $MgCl_2$, 5 mM Hepes, pH 7.6 with NaOH) for 1–7 days at 18°C.

For expression in mammalian cells, the channel cDNA was subcloned into pcDNA3 and transfected into human embryonic kidney cells (HEK-293T). HEK-293T cells were cultured in Dulbecco's Modified Eagle's Medium (DMEM) supplemented with fetal bovine serum (10%), glutamine (2 mM), penicillin (50 U ml^{-1}) and streptomycin (50 μg ml^{-1}; Gibco) in a humidified 37°C incubator with 95% air–5% CO_2. Cells were plated onto 12 mm

glass cover slips (Warner Instruments) coated with poly-D-lysine (20 μg ml^{-1}; Sigma) and collagen (100 μg ml^{-1}; BD Biosciences) in 24-well plates. HEK-293T cells were transiently transfected with cDNA using the calcium phosphate method. Briefly, cDNA (0.08 μg ml^{-1}) was

mixed in sterile de-ionized water with 0.25 M CaCl$_2$, then combined 1 : 1 with Hepes-buffered saline (280 mM NaCl, 10 mM KCl, 1.5 mM Na$_2$HPO$_4$, 12 mM glucose, 50 mM Hepes (pH 6.9 with ~1 N NaOH); 50 μl of this mixture was added to each well and incubated for 16–32 h.
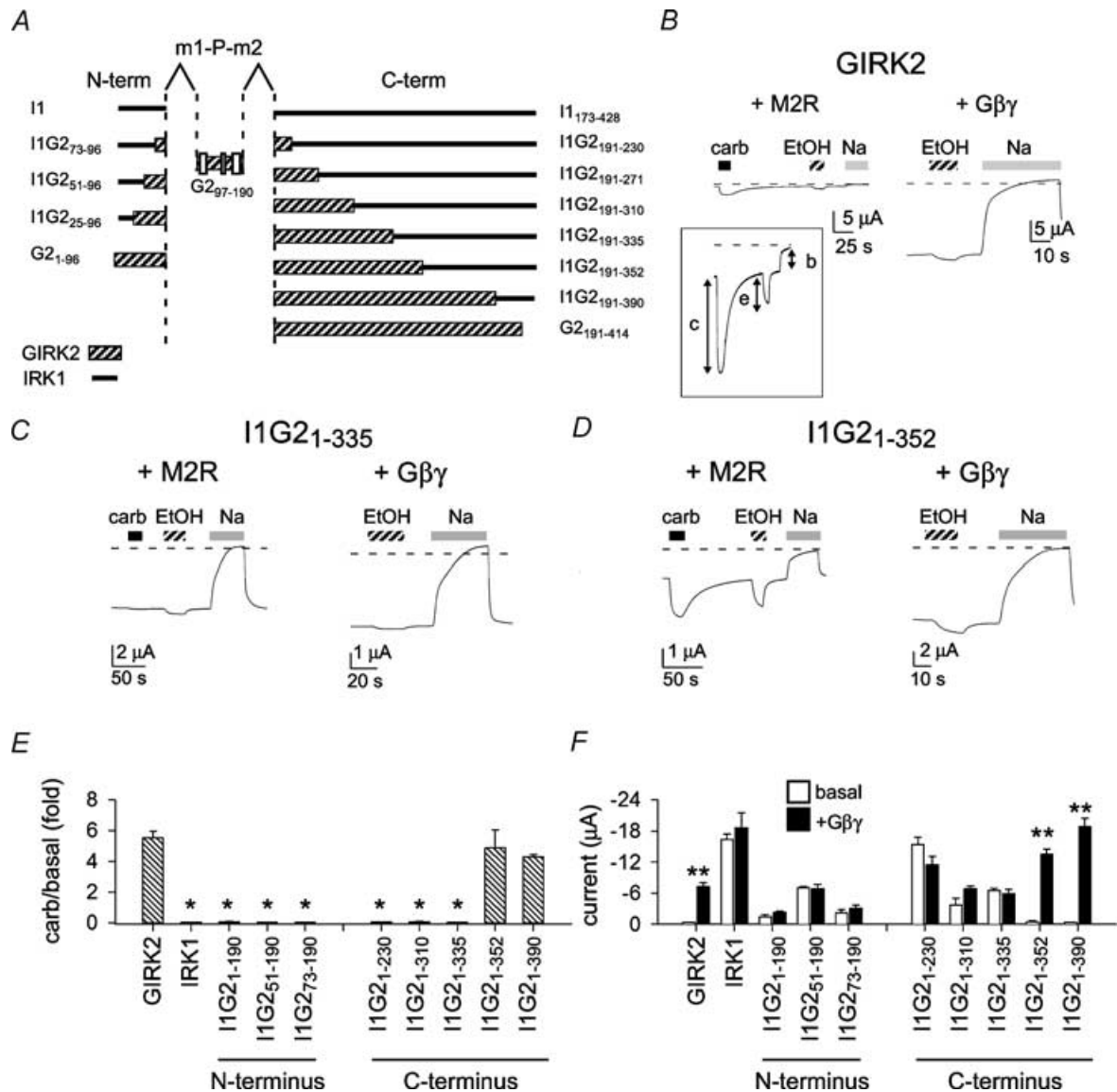

Figure 1. The amino acid segment that differs between chimeras I1G2$_{1-335}$ and I1G2$_{1-352}$ is important for G$_{\beta\gamma}$ activation

A, schematic diagram showing design of chimeras. Examples of macroscopic currents recorded from *Xenopus* oocytes injected with GIRK2 (*B*), I1G2$_{1-335}$ (*C*), I1G2$_{1-352}$ (*D*) cRNA and either the M2 muscarinic receptor (+ M2R), or G$_{\beta 1}$ and G$_{\gamma 2}$ subunits (+ G$_{\beta\gamma}$). GIRK2 shows both carbachol (carb)-activated and G$_{\beta\gamma}$-stimulated currents as well as ethanol (EtOH)-induced currents. I1G2$_{1-335}$ has a large basal current, but is not activated following carbachol stimulation. Currents were recorded with TEVC and perfused with 95 mM KCl, 95 mM KCl + 3 μM carbachol (filled bar), 95 mM KCl + 200 mM ethanol (hatched bar) or 95 mM NaCl (grey bar). The current in the presence of 95 mM NaCl represents the leakage current, and was used to measure the agonist-independent basal current. Holding potential was −80 mV. *E* and *F*, bar graphs show the carbachol-induced current normalized to the basal current (*E*) and the agonist-independent current in the absence and presence of G$_{\beta\gamma}$ subunits (*F*). *Significant difference from wild-type GIRK2 (*P* < 0.05). **Significant difference between basal and G$_{\beta\gamma}$ subunits (*P* < 0.05). *n* = 5–42.

Electrophysiology

Macroscopic currents were recorded from oocytes with a two-electrode voltage-clamp (TEVC) amplifier (Geneclamp 500, Axon Instruments), filtered at 0.05–2 kHz, digitized (0.1–2 kHz) with a Digidata 1200 A/D interface (Axon Instruments) and stored on a laboratory computer. Electrodes were filled with 3 M KCl and had resistances of 0.6–1 MΩ. Oocytes were perfused continuously with an extracellular solution containing 90 mM XCl (X = K^+ or Na^+), 2 mM $MgCl_2$ and 10 mM Hepes (pH 7.5 with ~5 mM XOH). The leakage current was determined using 95 mM Na^+ and subtracted directly from the current measured in 95 mM K^+. For ethanol activation, 100% ethanol was added directly to the 95 mM K^+ solution to give 200 mM ethanol (EtOH density = 0.7893 g ml^{-1}). A small chamber (3 mm × 15 mm) with fast perfusion was used to change the extracellular solution and was connected to earth via a 3 M KCl agarose bridge.

The whole-cell patch clamp technique (Hamill *et al.* 1981) was used to record macroscopic currents from HEK-293T cells. Borosilicate glass (Warner; P6165T) electrodes had resistances of 1–3 MΩ and were coated with Sylgard to reduce capacitance. Membrane currents were recorded with an Axopatch 200B (Axon Instruments) amplifier, adjusted electronically for cell capacitance and series resistance (80–100%), filtered at 2 kHz with an 8-pole Bessel filter, digitized at 5 kHz with a Digidata 1200 interface (Axon Instruments) and stored on a laboratory computer. Intracellular pipette solution contained (mM) 130 KCl, 20 NaCl, 5 EGTA, 2.56 K_2ATP, 5.46 $MgCl_2$ and 10 Hepes (pH 7.2 with ~14 mM KOH). With these ion concentrations there was ~140 mM K^+, 1.5 mM free Mg^{2+} and 2 mM Mg-ATP in the intracellular solution. Li_3-GTP (300 μM; RBI) was added fresh to the intracellular pipette solution to sustain the activation of GIRK channels. The external bath solution (20 mM K^+) contained (mM) 140 NaCl, 20 KCl, 0.5 $CaCl_2$, 2 $MgCl_2$ and 10 Hepes (pH 7.2). The osmolarity was 310–330 mosmol l^{-1}. Current–voltage relations were not corrected for the junction potential of ~4 mV, estimated using the Junction Potential Calculator (Axon Instruments).

Biochemistry

The C-terminal domains of GIRK2 (beginning with M191) and IRK1 (beginning with V179) were subcloned into pGEX2T (Amersham Pharmacia Biotech) using *Bam*H I and *Sma* I restriction sites engineered by PCR at the 5′ and 3′ ends of the C-terminal domains. The resulting GST-fused C-terminal domains were purified using standard procedures. $G_{\beta\gamma}$ binding to GST fusion proteins was measured as previously described (Huang *et al.* 1995) with the following modifications. Binding was performed for 45 min on ice and then each reaction sample was transferred onto a Cytosignal spin column. After three washes with 500 μl PBS–0.1% lubrol, the GST-fused proteins–$G_{\beta\gamma}$ complexes were eluted from the columns with 15 μl 2 × SDS sample buffer. Anti-G_β antibody (SC-20: Santa Cruz) and anti-GST antibody (Amersham Pharmacia) were used for Western blot analysis. Western blots were quantified using the 'gel' module in Image J (NIH software). For each blot, the optical density (OD) of the G_β band was divided by the OD for the GST band and then normalized to the GIRK2 for that experiment.

Immunocytochemistry

HEK-293T cells were cultured in DMEM containing 10% fetal bovine serum, 2.5 i.u. ml^{-1} penicillin–streptomycin, and 2 mM glutamine and transfected with HA-tagged constructs 24 h later using the calcium phosphate method. A haemagglutinin (HA) tag was inserted into the extracellular p-loop of mutant channels by subcloning the C-terminal mutation (via the *Bst* EII site) into HA-GIRK2, which was kindly provided by Chen *et al.* (2002). Cells were fixed 20–24 h after transfection by incubation in 1% paraformaldehyde for 30 min. The cells were washed two times with PBS and half were permeabilized by incubation with 0.25% Triton X-100 in PBS for 10 min. All cells were washed with PBS and incubated in blocking buffer (2% donkey serum and 2% IgG free bovine serum albumin in PBS) for 1 h at room temperature. The cells were incubated in the dark in Alexa488-conjugated anti-HA antibody (Covance) in blocking buffer (1 : 400) for 2 h at room temperature, washed three times with PBS and mounted onto glass coverslips with 1,4-diazabicyclo(2,2,2)octane (DABCO) in glycerol (*Slow Fade Light* Antifade Kit; Molecular Probes). Cells were imaged (0.35 μm slice thickness) using a Zeiss LSM 5 Pascal laser confocal microscope with a ×63 objective. To compare different mutants, the same gain, pin-hole and exposure time were used for all channels.

Analysis

All values are reported as mean ± S.E.M. Carbachol- ('c' in Fig. 1*B* inset) and ethanol-induced ('e') currents were expressed as a 'fold' increase over basal current ('b'), fold increase = c/b or e/b, respectively. One-way ANOVA followed by a *post hoc* Dunnett's test was used to test for statistical significance ($P < 0.05$), using GIRK2 as

control. A Bonferroni *post hoc* test was used to evaluate differences among mutants. In experiments examining the effect of expressing $G_{\beta\gamma}$ subunits, we used Student's two-tailed *t* test on the absolute current levels to compare basal *versus* coexpression with $G_{\beta\gamma}$ subunits. Distance between amino acids in the GIRK1 structure (PDB:1 N9P, Biological Unit) were measured using a Swiss-PDB viewer and displayed using Accelrys Viewerlite 5.0. The $G_{\beta\gamma}$ domains were defined based on the following studies. Huang *et al.* (1995, 1997) narrowed the $G_{\beta\gamma}$ binding domains to Q34–I86 in the N-terminal domain and V273–P462 in the C-terminal domain of GIRK1. Kunkel & Peralta (1995) identified T290–Y356 in GIRK1. Ivanina *et al.* (2003) demonstrated $G_{\beta\gamma}$ binding to F181–G254 and, to a lesser extent, G254–P370 of GIRK1 C-terminal domain. In GIRK2, $G_{\beta\gamma}$ binds to I46–L96 of the N-terminal and L310–E380 of the C-terminal domain of GIRK2 (Ivanina *et al.* 2003). He *et al.* (2002) demonstrated $G_{\beta\gamma}$ binding to N253–Y348 of GIRK4. Krapivinsky *et al.* (1997) identified two peptide sequences, M364–R383 of GIRK1 and S209–R225 of GIRK4, that exhibited potent inhibition of $G_{\beta\gamma}$ binding to native GIRK channels.

Results

C-terminal segment of GIRK2 channels implicated in $G_{\beta\gamma}$ activation

To localize the $G_{\beta\gamma}$ activation site(s) in GIRK2, 21 different chimeras of IRK1 and GIRK2 (using chimera I1G2$_{97-190}$ as the backbone) were constructed by systematically replacing 15–40 amino acid segments of IRK1 with the homologous amino acids from GIRK2 (Fig. 1*A*). I1G2$_{97-190}$ contained the hydrophobic core domain (m1-P-m2) from GIRK2 and N- and C-terminal domains from IRK1. I1G2$_{97-190}$ was shown previously to be K^+ selective and not gated by G proteins like IRK1 (Slesinger, 2001). In addition, chimera I1G2$_{97-190}$ preserved part of the G protein gate that was localized to the m2 transmembrane domain (Sadja *et al.* 2001; Yi *et al.* 2001). Each chimera cRNA was injected into *Xenopus* oocytes with either the cRNA for the M2 muscarinic receptor (M2R) or $G_{\beta1}$ and $G_{\gamma2}$ cRNAs. To evaluate channel function, we examined three parameters of channel activation. First, we measured the activation of current following stimulation of the M2 muscarinic receptor with carbachol (Fig. 1*B*, 'c' in inset); this activation relies on the endogenous G proteins and is $G_{\beta\gamma}$ sensitive. To account for possible changes in expression levels in oocytes, we expressed the carbachol-activated current as a function of the agonist-independent (basal) current. Second, we compared the amplitude of

basal current (Fig. 1*B*, 'b' in inset) in oocytes coexpressing the chimera with $G_{\beta\gamma}$ subunits ($+G_{\beta\gamma}$) with those coexpressing the chimera and M2R receptor. Coexpression of $G_{\beta\gamma}$ subunits in oocytes bypasses the endogenous G proteins, leading to the persistent $G_{\beta\gamma}$ activation of GIRK channels (Reuveny *et al.* 1994). We chose to express this as absolute current and used statistical analysis to assess whether $G_{\beta\gamma}$ subunits significantly enhanced the basal current. Third, we measured the amplitude of the inward current induced with 200 mM ethanol (Fig. 1*B*, 'e' in inset). Ethanol (EtOH) activates GIRK channels but inhibits IRK1 channels (Kobayashi *et al.* 1999; Lewohl *et al.* 1999; Zhou *et al.* 2001). Activation by ethanol does not require functional G proteins and therefore provides an important assessment of channel function for putative G protein-impaired mutants.

The GIRK2/IRK1 chimeras could be classified into three main groups: no current, $G_{\beta\gamma}$ sensitive, and $G_{\beta\gamma}$ impaired. Generally, chimeras containing the N-terminal domain of IRK1 and part or all of the C-terminal domain of GIRK2 failed to generate currents when expressed in oocytes (data not shown); these and other non-functional chimeras were not studied further (see Methods). Two chimeras (I1G2$_{1-352}$ and I1G2$_{1-390}$) were $G_{\beta\gamma}$ responsive and activated by ethanol, similar to GIRK2 (Fig. 1). The remaining chimeras (e.g. I1G2$_{1-190}$–I1G2$_{1-335}$) displayed moderate to large basal currents but little or no activation following stimulation of the muscarinic receptor (Fig. 1*E*). In addition, the basal current was not enhanced by coexpression with $G_{\beta\gamma}$ subunits (Fig. 1*F*). Thus, these chimeras appear to have impaired $G_{\beta\gamma}$ sensitivity. The change in $G_{\beta\gamma}$ sensitivity occurred between chimeras I1G2$_{1-335}$ and I1G2$_{1-352}$. To explore whether the agonist-independent current was $G_{\beta\gamma}$ sensitive for these two chimeras, we coinjected the cRNA for the C-terminal domain of βARK1 (βARK1-ct), which sequesters free $G_{\beta\gamma}$ subunits in oocytes (He *et al.* 1999). A $G_{\beta\gamma}$-sensitive basal current would be expected to be smaller in the presence of βARK1-ct. βARK-ct reduced the carbachol-activated current for GIRK2 and I1G2$_{1-352}$, indicating suppression of $G_{\beta\gamma}$ activity. The basal currents for I1G2$_{1-335}$ changed little in the presence of βARK1-ct, from $-6.6 \pm 0.6\,\mu$A ($n = 5$) to $-5.8 \pm 0.3\,\mu$A ($n = 5$) with βARK1-ct. Similarly, the basal current for I1G2$_{1-352}$ was not affected by βARK1-ct ($-0.45 \pm 0.19\,\mu$A ($n = 8$) *versus* $-0.46 \pm 0.22\,\mu$A ($n = 5$) with βARK1-ct. These results suggest the agonist-independent current is relatively insensitive to $G_{\beta\gamma}$ subunits, although we cannot rule out a small component of G protein-dependent activation.

To define the amino acids involved in $G_{\beta\gamma}$ activation better, we constructed point mutations in the region that

differed between I1G2$_{1-335}$ and I1G2$_{1-352}$. We focused on amino acids that are conserved among GIRK channels but differ from IRK1 (Fig. 2*A*). Five amino acids met this criterion, and each was changed from the amino acid in GIRK2 to the corresponding amino acid in IRK1. GIRK2$_{F388Y}$, GIRK2$_{T343F}$ and GIRK2$_{F348Y}$ all exhibited carbachol-induced currents that were comparable or larger than those of GIRK2 (Fig. 2*B* and *C*). Two mutations in GIRK2, GIRK2$_{L344E}$ and GIRK2$_{G347H}$, however, showed dramatically smaller carbachol-induced currents, 0.13-

fold and 0.54-fold increases over basal, respectively (compared to a 7.7-fold increase over basal for GIRK2). Despite the small carbachol response, both mutants showed a stimulated basal current when coexpressed with G$_{\beta\gamma}$ subunits as well as normal ethanol-induced currents (Fig. 2*B–E*). If L344E and G347H decrease the sensitivity of the mutant channel to G$_{\beta\gamma}$ subunits, then the agonist-activated response may be impaired because there is an insufficient amount of G$_{\beta\gamma}$ subunits generated during carbachol stimulation. In contrast, the high levels
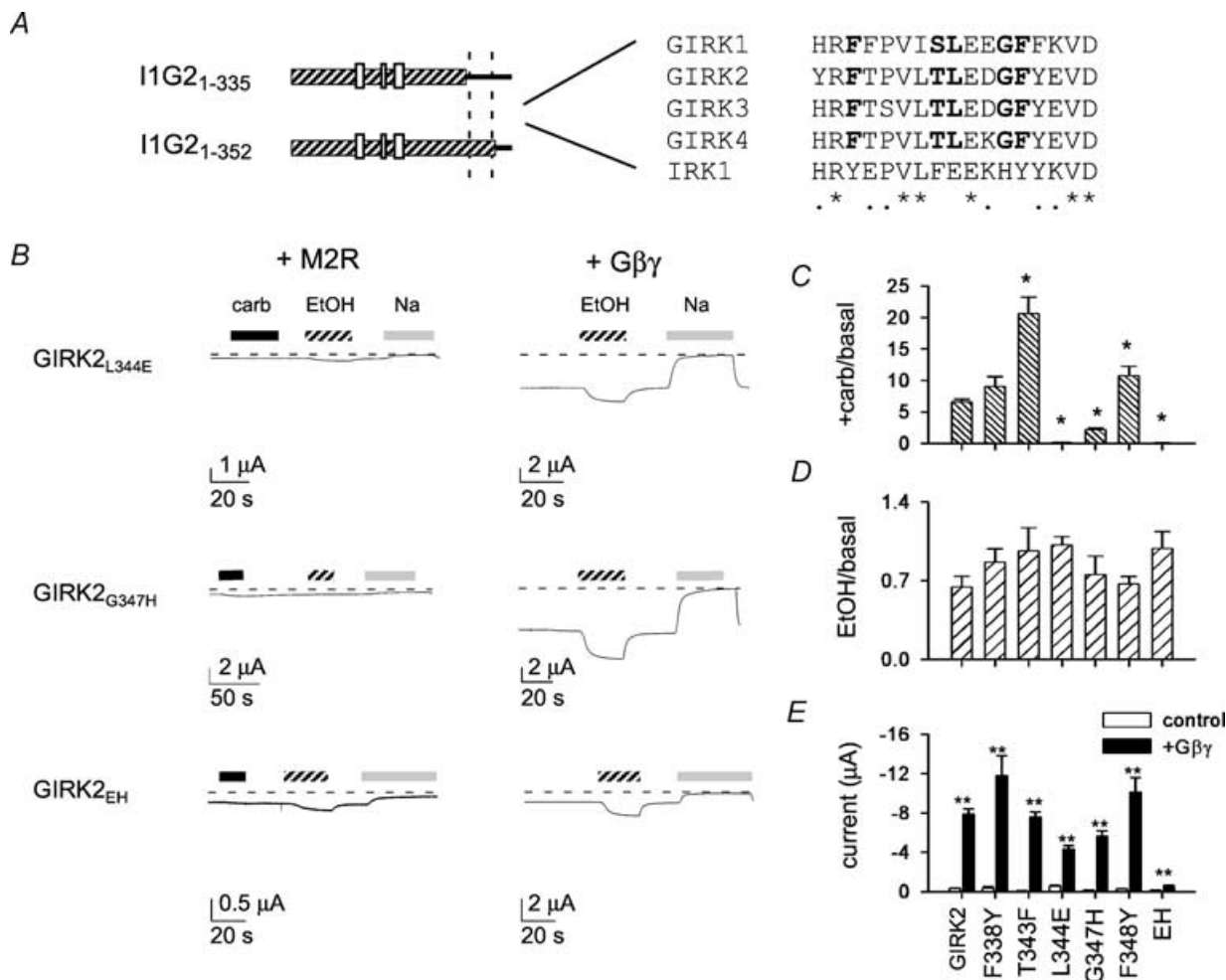

Figure 2. Mutation of two conserved amino acids in the C-terminal domain of GIRK2 reduces G$_{\beta\gamma}$ activation

A, sequence alignment of the amino acids in GIRK1, GIRK2, GIRK3, GIRK4 and IRK1. Amino acids that are conserved in GIRK family but differ from IRK1 are indicated in bold. Asterisk indicates 100% identity and small filled circles indicate conserved substitutions. *B–E*, oocytes were injected with cRNA for the indicated channel and with either the cRNA for M2R or G$_{\beta\gamma}$ subunits (*B*). Continuous recordings show the response to 0.3 μM carbachol (carb), 200 mM ethanol (EtOH) and 95 mM NaCl for GIRK2$_{L344E}$, GIRK2$_{G347H}$ and GIRK2$_{EH}$. Bar graphs show the average carbachol-induced current normalized to the basal current (*C*), the average ethanol-induced current normalized to the basal current (*D*) and the average G$_{\beta\gamma}$-induced and basal currents (*E*). Except for F338Y, the carbachol-induced currents for all other mutants are statistically different from GIRK2. None of the EtOH-activated currents is statistically different from GIRK2. All of the +G$_{\beta\gamma}$ currents are statistically larger than basal (*P* < 0.05). The increase for GIRK2$_{EH}$ (4-fold), however, is smaller than that for GIRK2 ($\sim$25-fold). *n* = 5–49.

of $G_{\beta\gamma}$ subunits that are present when $G_{\beta\gamma}$ subunits are coexpressed may be sufficient to activate the mutant channels.

We next tested for additivity of L344E and G347H effects on GIRK currents by introducing both mutations into GIRK2 (GIRK2$_{EH}$). Like the individual mutations, GIRK2$_{EH}$ exhibited a small basal current with a small increase ($\sim$0.02-fold) during carbachol stimulation. In contrast to the single point mutations, the $G_{\beta\gamma}$-stimulated currents for GIRK2$_{EH}$ were significantly reduced; the basal current for GIRK2$_{EH}$ was enhanced only $\sim$4-fold with coexpressed $G_{\beta\gamma}$ subunits, as compared to the $\sim$25-fold increase for GIRK2. Interestingly, the ethanol-induced currents for GIRK2$_{EH}$ were comparable to those of GIRK2 (Fig. 2D), suggesting that GIRK2$_{EH}$ retains ethanol sensitivity but has impaired $G_{\beta\gamma}$ activation. Thus, $G_{\beta\gamma}$ activation appears to be affected more severely in GIRK2$_{EH}$ than with either mutation alone.

Functional studies with $G_{\beta\gamma}$-impaired mutants expressed in HEK-293T cells

In *Xenopus* oocytes, GIRK channels can coassemble with an endogenous GIRK subunit (XIR) to produce heteromeric channels (Hedin *et al.* 1996). To eliminate any possible influence of XIR on the G protein sensitivity of the mutant channels studied in oocytes, we examined the $G_{\beta\gamma}$-impaired mutants expressed in HEK-293T cells using whole-cell patch clamp technique. Similar to oocytes, chimera I1G2$_{1-335}$ exhibited a large, agonist-independent current that was not increased further with carbachol (Figs 3B and 4A–C). By contrast, I1G2$_{1-352}$ showed both carbachol-induced and ethanol-induced currents, like GIRK2 (Fig. 4B and C). Thus, the $G_{\beta\gamma}$ sensitivity of chimeras I1G2$_{1-335}$ and I1G2$_{1-352}$ expressed in HEK-293T paralleled those observed in oocytes. Interestingly, we also observed a change in ethanol activation between chimeras I1G2$_{1-335}$ and I1G2$_{1-352}$ (Fig. 4C) in HEK-293T cells, which is similar to that reported by Lewohl *et al.* (1999).

We next examined the G protein sensitivity of GIRK2 point mutants expressed in HEK-293T cells. As in the oocytes, the GIRK2$_{L344E}$, GIRK2$_{G347H}$ and GIRK2$_{EH}$ all displayed small agonist-independent currents and markedly reduced carbachol-activated currents (Figs 3C and 4A and B). Ethanol (200 mM), on the other hand, activated the mutant GIRK2 channels, although the ethanol-activated current for G347H was dramatically smaller than control (Fig. 4C). The GIRK2 point mutants expressed in HEK-293T showed defects in $G_{\beta\gamma}$ activation similar to those observed in oocytes, indicating that

XIR did not contribute to the G protein phenotype. Because GIRK1 cannot express on the membrane surface in the absence of other GIRK subunits (Kennedy *et al.* 1996), we could now examine unequivocally whether GIRK2$_{EH}$ coassembles with GIRK1. Carbachol-activated currents were restored when GIRK1 was cotransfected with GIRK2$_{EH}$ (Figs 3D and 4B) and displayed the slow voltage-dependent activation kinetics typical of heteromultimers containing GIRK1 (Slesinger *et al.* 1996). Thus, GIRK2$_{EH}$ forms homotetramers as well as heterotetramers, like native GIRK2, indicating that the double (EH) mutation does not impair subunit assembly. Furthermore, the presence of one or more GIRK1 subunits in the tetramer appears to restore $G_{\beta\gamma}$ sensitivity.

The small basal and ethanol-activated currents for GIRK2$_{G347H}$ and GIRK2$_{EH}$ suggested that these mutants might express less efficiently than the other mutants in HEK-293T cells. To examine the surface expression of GIRK2 mutants, it was necessary to engineer an extracellular haemagglutinin (HA) epitope. The presence of the HA tag does not appear to alter the function of GIRK2 but may have some effect on trafficking (Chen *et al.* 2002; Ma *et al.* 2002). HEK-293T cells transfected with
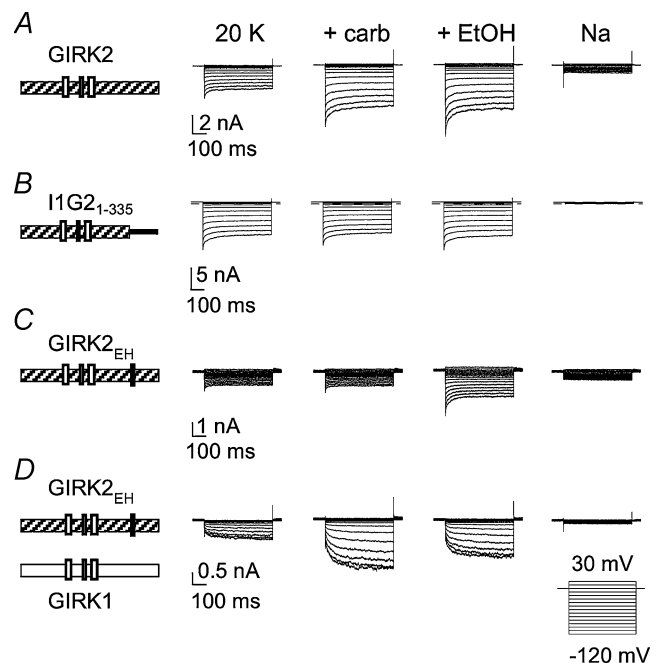

Figure 3. GIRK2$_{EH}$ expressed in HEK-293T cells has reduced carbachol activation but normal ethanol activation
HEK-293T cells were transiently transfected with cDNA for the M2R and either GIRK2 (*A*), I1G2$_{1-335}$ (*B*), GIRK2$_{EH}$ (*C*), or GIRK1 plus GIRK2$_{EH}$ (*D*) cDNA. Whole-cell patch clamp currents were elicited by voltage steps from −120 to 30 mV. Bath solutions contained 20 mM KCl (20 K) solution, 20 K + 0.3 μM carb, 20 K + 200 mM EtOH or 160 mM NaCl.

HA-GIRK2$_{L344E}$ showed intense membrane staining, which was the same or slightly more intense than that for wild-type HA-GIRK2 (Fig. 5*B* and *C*). By contrast, both HA-GIRK2$_{G347H}$ and HA-GIRK2$_{EH}$ expressed at lower levels on the membrane surface, though they were clearly detectable above the background staining of untransfected cells (Fig. 5*A*, *D* and *E*). In the presence of the L344E mutation, the G347H mutation appears to reduce the surface expression of the double mutant HA-GIRK2$_{EH}$. GIRK2$_{EH}$ expression, however, was recovered by coexpression with GIRK1 (Fig. 5*F*), consistent with the whole-cell patch clamp recordings (Fig. 4). If we normalize the carbachol-activated current to the amplitude of ethanol-activated current, which can serve as a measure of functional channels on the membrane surface, then I1G2$_{1-335}$, GIRK2$_{L344E}$ and GIRK2$_{EH}$ clearly show reduced carbachol activation (Fig. 4*D*). Taken together, these results suggest that some of the reduction in carbachol-

activated current in HEK-293T cells may be due to the lower expression levels for GIRK2$_{G347H}$ but not for GIRK2$_{L344E}$ and GIRK2$_{EH}$.

G$_{\beta\gamma}$ binding to C-terminal domains of GIRK2/IRK1 chimeras

We next examined whether L344 or G347 is important for the biochemical binding of G$_{\beta\gamma}$ to the channel. We used a coaffinity precipitation assay to measure the binding of G$_{\beta\gamma}$ subunits to fusion proteins containing the C-terminal domain of the channel (Fig. 6*A*). In contrast to previous studies examining G$_{\beta\gamma}$ binding with increasingly smaller fragments of the C-terminal domain of GIRK channels (Huang *et al.* 1995; He *et al.* 1999; Ivanina *et al.* 2003), we constructed GST fusion proteins that contained the entire cytoplasmic C-terminal domain of the chimera or the GIRK2 point mutant (Fig. 6*A*). As shown previously,
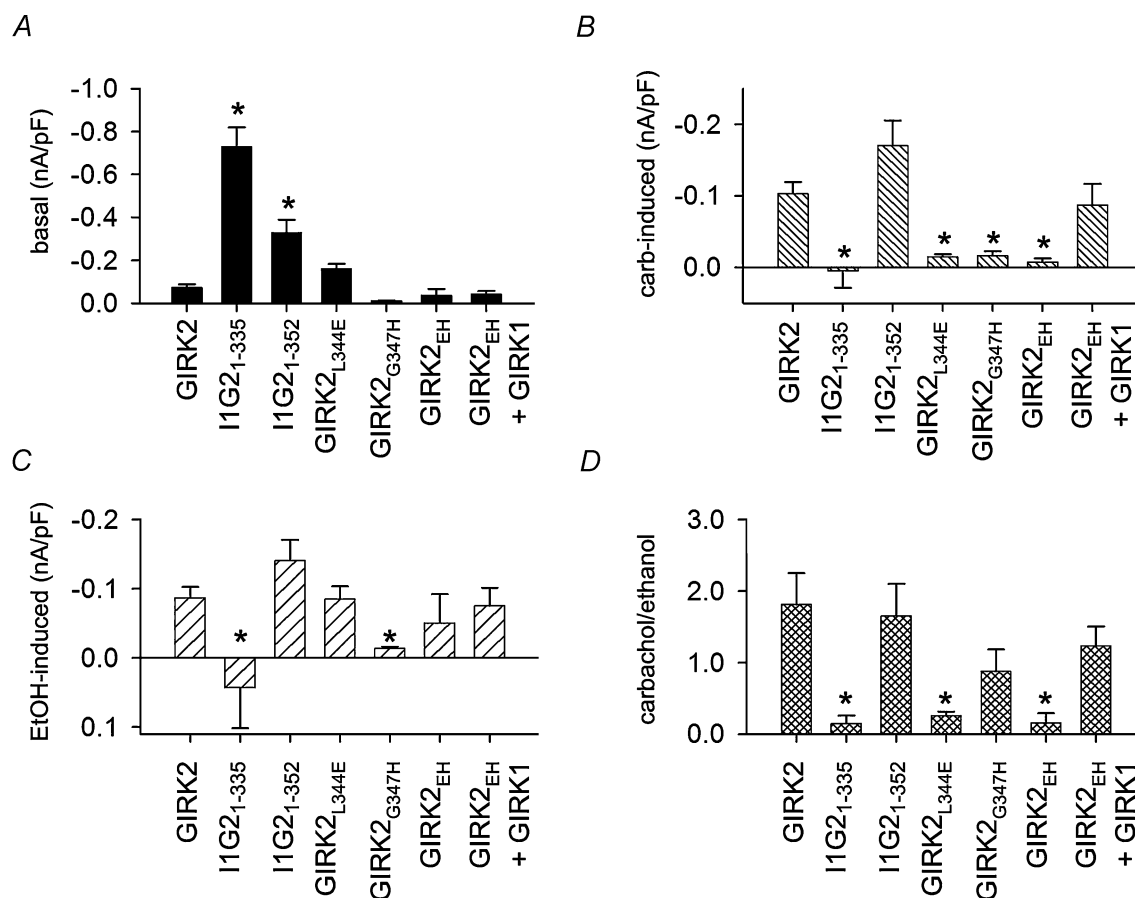

Figure 4. Summary of G protein sensitivity for mutants channels expressed in HEK-293T cells
Bar graphs show the agonist-independent (*A*), the carbachol-induced (*B*), and the ethanol-induced (*C*) current density for each mutant. Using the ethanol-activated current as a measure of channel expression, the carbachol-activated current was normalized to the amplitude of ethanol-activated current (*D*). *Significant difference from GIRK2 ($P < 0.05$). $n = 5$–18.

the C-terminal domain of GIRK2 but not IRK1 binds $G_{\beta\gamma}$ subunits (Huang *et al.* 1997). Surprisingly, fusion proteins containing the C-terminal domain from the different chimeras all exhibited $G_{\beta\gamma}$ binding similar to GIRK2 (Fig. 6*B*). Chimeras containing either the proximal (GST-I1G2$_{181-230}$) or distal (GST-I1G2$_{353-414}$) region of GIRK2 exhibited similar $G_{\beta\gamma}$ binding that was clearly greater than the $G_{\beta\gamma}$ binding to the GST alone or the C-terminal domain of IRK1. By contrast, the $G_{\beta\gamma}$ binding to the C-terminal domain of GIRK2$_{EH}$ appeared slightly reduced (Fig. 6*C*). To quantify these possible differences in $G_{\beta\gamma}$ binding, we measured the optical density (OD) of the G_β band, divided by the OD for the GST band and then normalized to the $G_{\beta\gamma}$ binding for GIRK2 (Fig. 6*D*). Compared to the full-length C-terminal domain of GIRK2 (GST-G2$_{191-414}$), only GST-G2$_{L344E}$ and GST-I1$_{173-428}$ showed significantly less $G_{\beta\gamma}$ binding (Fig. 6*D*). However, $G_{\beta\gamma}$ binding to GST-G2$_{L344E}$ was not statistically different from GST-G2$_{G347H}$ or GST-G2$_{EH}$. Taken together, the electrophysiological and biochemical experiments suggest that L344 plays a major role in $G_{\beta\gamma}$ activation and, to a lesser extent, in $G_{\beta\gamma}$ binding.

Discussion

Important role for βL–βM loop in $G_{\beta\gamma}$ activation

We first evaluated in *Xenopus* oocytes the ability of mutant GIRK channels to be activated through stimulation of the m2 muscarinic receptor as well as by coexpression with $G_{\beta\gamma}$ subunits. In the latter case, we assume that the concentration of free $G_{\beta\gamma}$ is significantly higher as compared to the $G_{\beta\gamma}$ liberated during stimulation of the m2 muscarinic receptor. This supposition seems justified since the carbachol-activated currents were on average significantly smaller than the basal currents recorded in oocytes coexpressing $G_{\beta\gamma}$ subunits. We found that GIRK2 channels containing either the L344E or G347H mutation exhibited dramatically smaller carbachol-activated currents but were still activated by coexpressed $G_{\beta\gamma}$ subunits. Combining the two mutations (GIRK2$_{EH}$) produced channels that were unresponsive to muscarinic receptor stimulation and now showed little enhancement with coexpressed $G_{\beta\gamma}$ subunits. Electrophysiological recordings obtained in HEK-293T cells also supported the conclusion that L344E and, to a lesser extent, G347H, were important for $G_{\beta\gamma}$ activation. Interestingly,
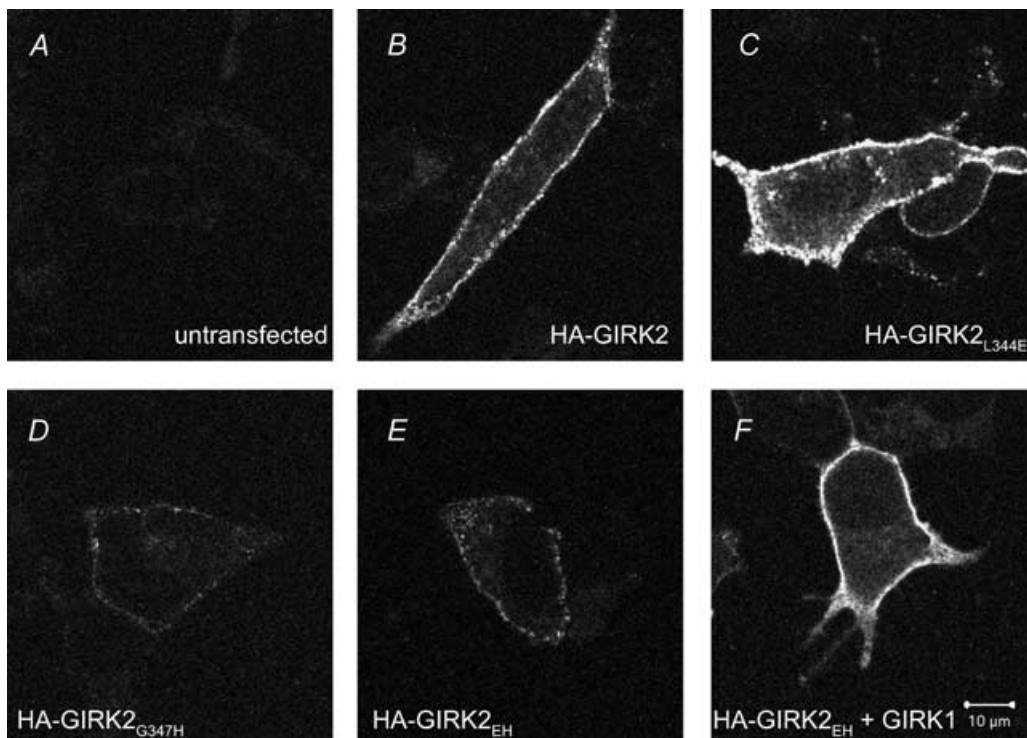

Figure 5. Immunostaining of HA-tagged GIRK2 channels expressed in HEK-293T cells
HEK-293T cells were transfected with the channel cDNA indicated in the figure. *A–F*, surface localization was revealed by immunostaining non-permeabilized cells using an Alexa488 conjugated anti-HA antibody. Images were obtained with a laser confocal microscope, using the same gain, slice thickness (0.35 μm), pin-hole and exposure time.

L344 and G347 are both conserved among the different types of GIRK channels but differ in G protein-insensitive inward rectifiers (see Supplementary Material available online), suggesting an important functional role for these amino acids. Assuming the three-dimensional structure of the GIRK2 cytoplasmic domains is the same as that of GIRK1 (Nishida & MacKinnon, 2002), L344 and G347 would be located in an exposed loop (βL–βM) facing the intracellular milieu (see Fig. 7*B*).

We examined the surface labelling of HA-tagged channels expressed in HEK-293T cells to determine whether the smaller $G_{\beta\gamma}$-activated currents could be explained by decreased surface expression. The expression of GIRK2$_{L344E}$ was the same as, or slightly higher than, that

of wild-type GIRK2 when expressed in HEK-293T cells. Consistent with this, the functional response to ethanol for GIRK2$_{L344E}$, which activates GIRK channels through a G protein-independent mechanism (Kobayashi *et al.* 1999; Lewohl *et al.* 1999; Zhou *et al.* 2001), was comparable with that of wild-type GIRK2 channels. Cells transfected with either HA-GIRK2$_{G347H}$ or HA-GIRK2$_{EH}$ showed weak plasma membrane staining relative to HA-GIRK2. However, normalizing the carbachol-activated currents to the amplitude of ethanol-activated currents, which can serve as an indicator of surface expression, suggests that $G_{\beta\gamma}$ activation is impaired in both GIRK2$_{L344E}$ and the double mutant, GIRK2$_{EH}$. Perhaps G347H amplifies the $G_{\beta\gamma}$ deficiency of L344E in the double mutant. Additional
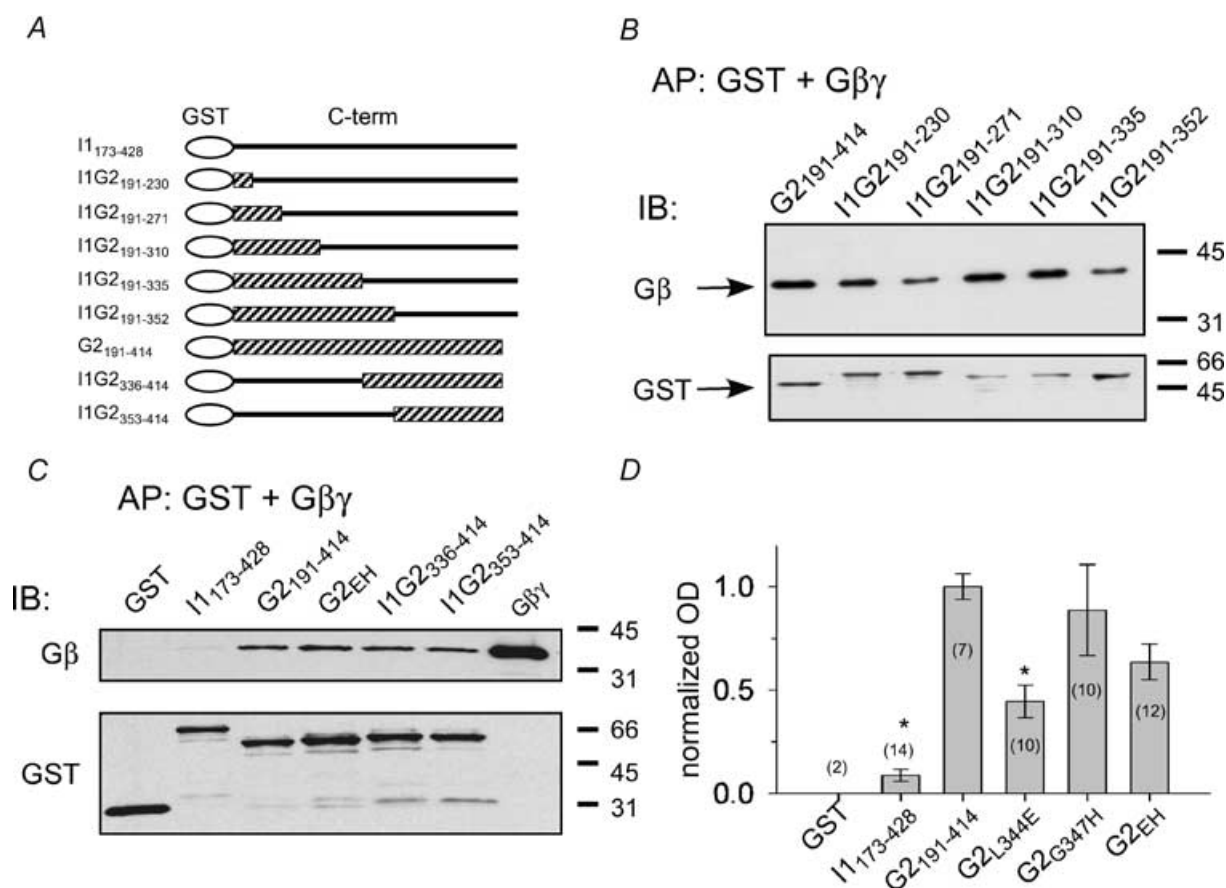

Figure 6. Mutations in βL–βM loop of GIRK2 show variable changes in $G_{\beta\gamma}$ binding
In vitro coaffinity precipitation (AP) assays were used to measure the $G_{\beta\gamma}$ binding to GST fusion proteins containing the C-terminal domain of the wild-type or mutant channel. *A*, schematic diagram of GST fusion proteins. *B*, GST fusion proteins (200 nM) were mixed with purified bovine brain $G_{\beta\gamma}$ subunits (40 nM). Immuno-blot (IB) using antibody against G_β (upper panel) and, after stripping the blot, against GST (lower panel). All chimeras showed some $G_{\beta\gamma}$ binding. *C*, $G_{\beta\gamma}$ binding assay for GST, GST-I1$_{173-428}$, GST-G2$_{191-414}$, GST-G2$_{EH}$, GST-G2$_{336-414}$ and GST-G2$_{353-414}$. *D*, quantification of $G_{\beta\gamma}$ binding. The optical density (OD) of the G_β band was divided by the OD of the GST band, and then normalized to the GIRK2 for each blot (*n* indicated in parentheses). *Statistical difference from GST-G2$_{191-414}$ (*P* < 0.05, ANOVA followed by *post hoc* Bonferroni test). GST-G2$_{L344E}$ is not statistically different from GST-G2$_{G347H}$ or GST-G2$_{EH}$.
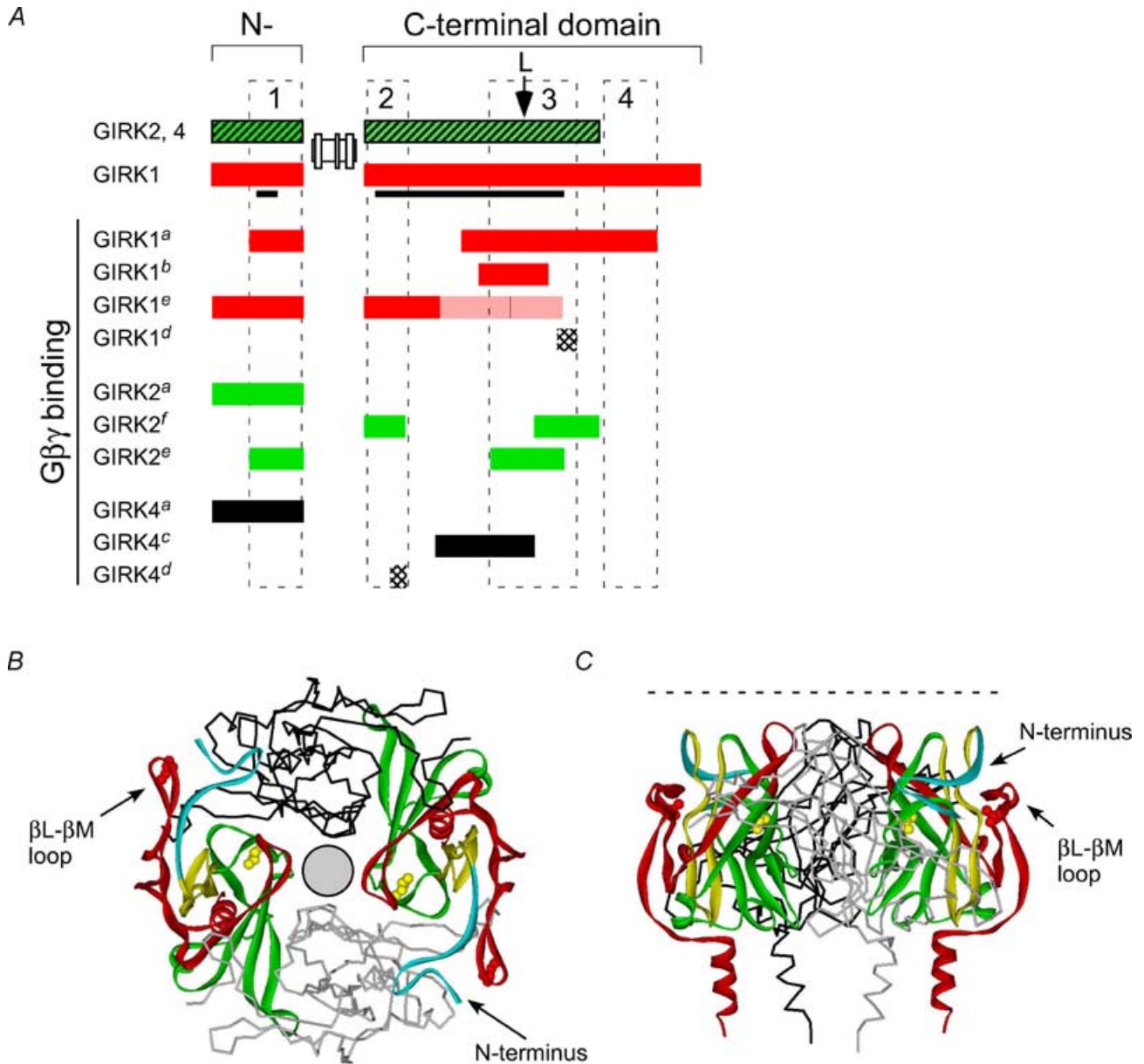
Figure 7. Multiple sites for G$_{\beta\gamma}$ interaction with GIRK channels: a role for the βL–βM loop in G$_{\beta\gamma}$ activation

A, alignment of the G$_{\beta\gamma}$ binding domains in the N- and C-terminal domains of GIRK channel identified in the following studies: [a]Huang *et al.* 1995, 1997; [b]Kunkel & Peralta, 1995; [c]He *et al.* 1999, 2002; [d]Krapivinsky *et al.* 1998; [e]Ivanina *et al.* 2003; and [f]this study (see Methods for details). Filled bars (red, green, black): regions binding G$_{\beta\gamma}$ subunits. Shaded red bar: regions showing less G$_{\beta\gamma}$ binding. Stippled bars: peptide competing for G$_{\beta\gamma}$ binding. Arrow marks position of the leucine in the βL–βM loop. The GIRK1 sequence included in 3-D structure is indicated by the black line. Three G$_{\beta\gamma}$ binding domains are drawn to indicate regions of most overlap for G$_{\beta\gamma}$ binding, along with a region unique to GIRK1 (see text for details). *B*, three putative G$_{\beta\gamma}$ segments are highlighted in the GIRK1 structure (Nishida & MacKinnon, 2002). Model shows four subunits arranged around a pore (circle), with two subunits highlighting G$_{\beta\gamma}$ domains: region 1 (R43–E63, turquoise), region 2 (R190–R219, yellow) and region 3 (E300–P370, red). The amino acid sequence between regions 2 and 3 (green) has also been implicated in G$_{\beta\gamma}$ binding. Region 4 is unique to GIRK1 and is not present in the structure. Note proximity of the N-terminal domain to the βL–βM loop. Two amino acids, L262 (yellow, He *et al.* 2002) and L333E (red) are highlighted in the structure. *C*, side view of the same structure. Dashed line indicates approximate position of the cytoplasmic side of the plasma membrane.

mutagenesis studies are required to determine the precise role of G347H in surface expression and/or $G_{\beta\gamma}$ activation.

The L344 in the βL–βM loop of GIRK2 has been implicated previously in other GIRK channels. In a study of GIRK4, He *et al.* (1999) discovered that L339E in GIRK4 (homologous to GIRK2$_{L344E}$) impaired agonist-induced activation, similar to GIRK2$_{L344E}$ and GIRK2$_{EH}$. In addition to a loss of agonist-activated current, GIRK4*$_{L339E}$ exhibited a large, agonist-independent current that was not increased by coexpression with $G_{\beta\gamma}$ subunits (He *et al.* 1999). The basal current was suppressed by coexpression of βARK1-ct or G_α G protein, however, leading He *et al.* (1999) to postulate that the agonist-induced current and $G_{\beta\gamma}$-dependent basal current are generated by two different $G_{\beta\gamma}$ binding sites on the channel; a high affinity site that produces the agonist-independent current and is saturated under basal conditions, and a low affinity $G_{\beta\gamma}$ binding site that is occupied following agonist activation. For generating large, agonist-independent currents for homomeric GIRK4 channels, He *et al.* (1999) introduced a mutation in the pore of GIRK4 (GIRK4*$_{S143T}$) to promote the expression of the homomultimer (Chan *et al.* 1996; He *et al.* 1999). Although the S143T mutation has no effect on single-channel kinetics, it is unclear how the mutation leads to larger currents. Interestingly, Peleg *et al.* (2002) found that GIRK channels expressed at high levels in oocytes leads to large, agonist-independent currents with small receptor-activated currents, due to a limiting supply of G_α subunits. In our study, the expression of GIRK2 in oocytes or HEK-293T cells did not generate an agonist-independent current that was large enough to reliably test the effect of βARK1-ct. In a recent study by Ivanina *et al.* (2003), GIRK1$_{L333E}$/GIRK2$_{L344E}$ heteromultimers expressed in oocytes displayed small, agonist-independent and agonist-activated currents, similar to our results. Collectively, these studies provide convincing evidence that the leucine in the βL–βM loop plays an important functional role in $G_{\beta\gamma}$ activation.

How does mutating the leucine in the βL–βM loop account for the change in $G_{\beta\gamma}$ activation? One possibility is that the binding of $G_{\beta\gamma}$ subunits to the channel is altered. The effect of the leucine-to-glutamate mutation on the biochemical binding of $G_{\beta\gamma}$, however, is more equivocal. He *et al.* (1999) reported an ∼60% decrease in $G_{\beta\gamma}$ binding to the C-terminal domain of GIRK4$_{L339E}$. However, $G_{\beta\gamma}$ binding was also reduced for GIRK4$_{L268I}$, which had a defective $G_{\beta\gamma}$-dependent basal current (He *et al.* 2002). Using *in vitro* translated ^{35}S-labelled $G_{\beta\gamma}$ to measure binding to GIRK channels, Ivanina *et al.* (2003) observed

a 30–40% decrease in binding to the C-terminal domain of GIRK1$_{L333E}$ but no detectable change in $G_{\beta\gamma}$ binding to the C-terminal domain of GIRK2$_{L344E}$. In our experiments with purified $G_{\beta\gamma}$ subunits, L344E exhibited ∼60% less $G_{\beta\gamma}$ binding but the double mutant (GIRK2$_{EH}$) and the chimeric channel (I1G2$_{1-335}$), which both exhibited defective $G_{\beta\gamma}$ activation, were not statistically different from control. One complication to the binding studies is that $G_{\beta\gamma}$ subunits bind to multiple regions in the C-terminal domain (see below), thereby potentially masking changes in $G_{\beta\gamma}$ binding.

Even with a twofold decrease in $G_{\beta\gamma}$ binding, it may appear difficult to reconcile this small change with a major loss of agonist-activated and $G_{\beta\gamma}$-stimulated currents. A limitation to the $G_{\beta\gamma}$ binding assay, however, is that $G_{\beta\gamma}$ binding is measured *in vitro* with a fusion protein that lacks the transmembrane domains. If we consider GIRK channels to be allosteric proteins, then the affinity for $G_{\beta\gamma}$ subunits may change depending on the state of the channel (Changeux & Edelstein, 1998). Thus, it remains possible that $G_{\beta\gamma}$ binding is altered more dramatically in the context of the intact mutant channel. On the other hand, $G_{\beta\gamma}$ activation is highly cooperative, requiring the binding of multiple $G_{\beta\gamma}$ dimers to the channel (Corey & Clapham, 2001). Thus, a subtle mutation in all four subunits may alter the cooperativity of $G_{\beta\gamma}$ activation and lead to reduced $G_{\beta\gamma}$ activation. Finally, mutations in the βL–βM loop may interfere with the coupling of $G_{\beta\gamma}$ binding to the channel's activation gate. Future studies will clarify the link between $G_{\beta\gamma}$ binding and channel activation.

$G_{\beta\gamma}$ binding sites mapped on the GIRK1 structure

In addition to the βL–βM loop, several other regions in the C-terminal domain of GIRK channels have been implicated in $G_{\beta\gamma}$ binding. We compared the $G_{\beta\gamma}$ binding domains implicated in this and previous studies, and searched for regions of greatest overlap. Based on this criterion, we identified three general regions in GIRK channels important for $G_{\beta\gamma}$ binding (Fig. 7*A*, see Methods for details). Region 1 contains part of the N-terminal domain. Defining the regions in the C-terminal domain was more difficult and somewhat subjective, since $G_{\beta\gamma}$ sites appear to be distributed over the entire C-terminal domain. We suggest that two general regions, a proximal (region 2) and middle (region 3) C-terminal segment of GIRK1–4, can account for most of the overlap in $G_{\beta\gamma}$ binding sites. Region 3 encompasses the βL–βM loop and surrounding amino acids. A fourth region (region 4) may exist that is unique to the distal end of GIRK1.

Mapping these putative $G_{\beta\gamma}$ binding segments onto the three-dimensional structure of GIRK1 reveals that they are clustered on the outer edge of the tetrameric channel, away from the central pore, and well positioned to interact with $G_{\beta\gamma}$ subunits (Fig. 7B). Further refinement of the $G_{\beta\gamma}$ sites on GIRK channels will require the structural determination of a complex of $G_{\beta\gamma}$ subunits and GIRK cytoplasmic domains, as well as incoporation of the G_{α} binding site (Huang *et al.* 1995) and PIP_2 sites (Huang *et al.* 1998; Sui *et al.* 1998).

The propinquity of the βL–βM loop to the N-terminal domain suggests a testable model for $G_{\beta\gamma}$ activation. The βL–βM loop is situated within 4 Å (Q44–G336 distance is 3.6 Å) of the N-terminal domain. Thus, $G_{\beta\gamma}$ binding may alter the interaction between the βL–βM loop of one subunit with the N-terminal domain of the neighbouring subunit. Strengthening the bonds within the loop and the N-terminal domain might interfere with $G_{\beta\gamma}$ activation. Using the Swiss-Pdb Viewer program to model mutations in GIRK1, the side-chain of the glutamate (L333E) could form hydrogen bonds with the backbone of E334, E335 and F337, within the βL–βM loop. The side-chain of the histidine (G336H) could form a hydrogen bond with the Q44 located in the N-terminal domain. Based on this model, it may be possible to create a mutation that will rescue the $G_{\beta\gamma}$ defect of L344E/G347H. Several lines of evidence support an important role for coupling between the N- and C-terminal domains in other types of inward rectifiers during channel activation. First, the N-terminal domain of GIRK binds $G_{\beta\gamma}$ subunits and interacts cooperatively with the C-terminal domain (Huang *et al.* 1997). Second, Schulte *et al.* (1998) found that cysteines in the N- and C-terminal domains of ROMK1 (Kir1.1) were modified only in the closed state, indicating a conformational change in the cytoplasmic domains. Finally, mutations in the N-terminal domain of K_{ATP} channel subunit (Kir6.2) disrupt the binding of the N-terminal domain to the C-terminal domain (Tucker & Ashcroft, 1999).

References

Blednov YA, Stoffel M, Chang SR & Harris RA (2001). Potassium channels as targets for ethanol: studies of G-protein-coupled inwardly rectifying potassium channel 2 (GIRK2) null mutant mice. *J Pharmacol Exp Ther* **298**, 521–530.

Chan KW, Sui JL, Vivaudou M & Logothetis DE (1996). Control of channel activity through a unique amino acid residue of a G protein-gated inwardly rectifying K$^+$ channel subunit. *Proc Natl Acad Sci U S A* **93**, 14193–14198.

Changeux J-P & Edelstein S (1998). Allosteric receptors after 30 years. *Neuron* **21**, 959–980.

Chen L, Kawano T, Bajic S, Kaziro Y, Itoh H, Art JJ, Nakajima Y & Nakajima S (2002). A glutamate residue at the C terminus regulates activity of inward rectifier K$^+$ channels: Implication for Andersen's syndrome. *Proc Natl Acad Sci U S A* **99**, 8430–8435.

Corey S & Clapham DE (2001). The stoichiometry of G$\beta\gamma$ binding to G-protein-regulated inwardly rectifying K$^+$ channels (GIRKs). *J Biol Chem* **276**, 11409–11413.

Doupnik CA, Davidson N & Lester HA (1995). The inward rectifier potassium channel family. *Curr Opin Neurobiol* **5**, 268–277.

Finley M, Arrabit C, Fowler C & Slesinger PA (2003). Identification of a conserved C-terminal region of Kir3 important for G$\beta\gamma$ activation. In *Biophysical Society 47th Annual Meeting*. Biophysical Society, San Antonio, Texas.

Hamill OP, Marty A, Neher E, Sakmann B & Sigworth FJ (1981). Improved patch-clamp techniques for high-resolution current recording from cells and cell-free membrane patches. *Pflügers Arch* **391**, 85–100.

He C, Yan X, Zhang H, Mirshahi T, Jin T, Huang A & Logothetis DE (2002). Identification of critical residues controlling G protein-gated inwardly rectifying K$^+$ channel activity through interactions with the $\beta\gamma$ subunits of G proteins. *J Biol Chem* **277**, 6088–6096.

He C, Zhang H, Mirshahi T & Logothetis DE (1999). Identification of a potassium channel site that interacts with G protein $\beta\gamma$ subunits to mediate agonist-induced signaling. *J Biol Chem* **274**, 12517–12524.

Hedin KE, Lim NF & Clapham DE (1996). Cloning of a Xenopus laevis inwardly rectifying K$^+$ channel subunit that permits GIRK1 expression of IKACh currents in oocytes. *Neuron* **16**, 423–429.

Hille B (1992). *Ionic Channels of Excitable Membranes*. Sinauer Assoc, Sunderland, MA, USA.

Ho IH & Murrell-Lagnado RD (1999). Molecular determinants for sodium-dependent activation of G protein-gated K$^+$ channels. *J Biol Chem* **274**, 8639–8648.

Huang C-L, Feng S & Hilgemann DW (1998). Direct activation of inward rectifier potassium channels by PIP2 and its stabilization by G$\beta\gamma$. *Nature* **391**, 803–806.

Huang CL, Jan YN & Jan LY (1997). Binding of the G protein $\beta\gamma$ subunit to multiple regions of G protein-gated inward-rectifying K$^+$ channels. *FEBS Lett* **405**, 291–298.

Huang CL, Slesinger PA, Casey PJ, Jan YN & Jan LY (1995). Evidence that direct binding of G$\beta\gamma$ to the GIRK1 G protein-gated inwardly rectifying K$^+$ channel is important for channel activation. *Neuron* **15**, 1133–1143.

Inanobe A, Morishige K-I, Takahashi N, Ito H, Yamada M, Takumi T, Nishina H, Takahashi K, Kanaho Y, Katada T & Kurachi Y (1995). G$\beta\gamma$ directly binds to the carboxyl terminus of the G protein-gated muscarinic K$^+$ channel, GIRK1. *Biochem Biophys Res Commun* **212**, 1022–1028.

Inanobe A, Yoshimoto Y, Horio Y, Morishige K-I, Hibino H, Matsumoto S, Tokunaga Y, Maeda T, Hata Y, Takai Y & Kurachi Y (1999). Characterization of G-protein-gated K$^+$ channels composed of Kir3.2 subunits in dopaminergic neurons of the substantia nigra. *J Neurosci* **19**, 1006–1017.

Ivanina T, Rishal I, Varon D, Mullner C, Frohnwieser-Steinecke B, Schreibmayer W, Dessauer CW & Dascal N (2003). Mapping the G$\beta\gamma$-binding sites in GIRK1 and GIRK2 subunits of the G protein-activated K$^+$ channel. *J Biol Chem* **278**, 29174–29183.

Jelacic TM, Kennedy ME, Wickman K & Clapham DE (2000). Functional and biochemical evidence for G-protein-gated inwardly rectifying K$^+$ (GIRK) channels composed of GIRK2 and GIRK3. *J Biol Chem* **275**, 36211–36216.

Kennedy ME, Nemec J & Clapham DE (1996). Localization and interaction of epitope-tagged GIRK1 and CIR inward rectifier K$^+$ channel subunits. *Neuropharmacology* **35**, 831–839.

Kobayashi T, Ikeda K, Kojima H, Niki H, Yano R, Yoshiola T & Kumanishi T (1999). Ethanol opens G-protein-activated inwardly rectifying K$^+$ channels. *Nat Neurosci* **2**, 1091–1097.

Krapivinsky G, Kennedy ME, Nemec J, Medina I, Krapivinsky L & Clapham DE (1998). G$_{\beta\gamma}$ binding to GIRK4 subunit is critical for G protein-gated K$^+$ channel activation. *J Biol Chem* **273**, 16946–16952.

Kubo Y, Baldwin TJ, Jan YN & Jan LY (1993*a*). Primary structure and functional expression of a mouse inward rectifier potassium channel. *Nature* **362**, 127–133.

Kubo Y, Reuveny E, Slesinger PA, Jan YN & Jan LY (1993*b*). Primary structure and functional expression of a rat G-protein-coupled muscarinic potassium channel. *Nature* **364**, 802–806.

Kunkel MT & Peralta EG (1995). Identification of domains conferring G protein regulation on inward rectifier potassium channels. *Cell* **83**, 443–449.

Lesage F, Duprat F, Fink M, Guillemare E, Coppola T, Lazdunski M & Hugnot JP (1994). Cloning provides evidence for a family of inward rectifier and G-protein coupled K$^+$ channels in the brain. *FEBS Lett* **353**, 37–42.

Lewohl JM, Wilson WR, Mayfield RD, Brozowski SJ, Morrisett RA & Harris RA (1999). G-protein-coupled inwardly rectifying potassium channels are targets of alcohol action. *Nat Neurosci* **2**, 1084–1090.

Liao YJ, Jan YN & Jan LY (1996). Heteromultimerization of G-protein-gated inwardly rectifying K$^+$ channel proteins GIRK1 and GIRK2 and their altered expression in weaver brain. *J Neurosci* **16**, 7137–7150.

Logothetis DE, Kurachi Y, Galper J, Neer EJ & Clapham DE (1987). The $\beta\gamma$ subunits of GTP-binding proteins activate the muscarinic K$^+$ channel in heart. *Nature* **325**, 321–326.

Ma D, Zerangue N, Raab-Graham K, Fried SR, Jan YN & Jan LY (2002). Diverse trafficking patterns due to multiple traffic motifs in G protein-activated inwardly rectifying potassium channels from brain and heart. *Neuron* **33**, 715–729.

Nishida M & MacKinnon R (2002). Structural basis of inward rectification. Cytoplasmic pore of the G protein-gated inward rectifier GIRK1 at 1.8 A resolution. *Cell* **111**, 957–965.

Peleg S, Varon D, Ivanina T, Dessauer CW & Dascal N (2002). Gαi controls the gating of the G protein-activated K$^+$ channel, GIRK. *Neuron* **33**, 87–99.

Petit-Jacques J, Sui JL & Logothetis DE (1999). Synergistic activation of G protein-gated inwardly rectifying potassium channels by the $\beta\gamma$ subunits of G proteins and Na$^+$ and Mg^{2+} ions. *J General Physiol* **114**, 673–684.

Reuveny E, Slesinger PA, Inglese J, Morales JM, Iniguez-Lluhi JA, Lefkowitz RJ, Bourne HR, Jan YN & Jan LY (1994). Activation of the cloned muscarinic potassium channel by G protein $\beta\gamma$ subunits. *Nature* **370**, 143–146.

Sadja R, Smadja K, Alagem N & Reuveny E (2001). Coupling G$\beta\gamma$-dependent activation to channel opening via pore elements in inwardly rectifying potassium channels. *Neuron* **29**, 669–680.

Schulte U, Hahn H, Wiesinger H, Ruppersberg JP & Fakler B (1998). pH-dependent gating of ROMK (Kir1.1) channels involves conformational changes in both N and C termini. *J Biol Chem* **273**, 34575–34579.

Signorini S, Liao YJ, Duncan SA, Jan LY & Stoffel M (1997). Normal cerebellar development but susceptibility to seizures in mice lacking G protein-coupled, inwardly rectifying K$^+$ channel GIRK2. *Proc Natl Acad Sci U S A* **94**, 923–927.

Slesinger PA (2001). Ion selectivity filter regulates local anesthetic inhibition of G protein-gated inwardly rectifying K$^+$ channels. *Biophys J* **80**, 707–718.

Slesinger PA, Patil N, Liao YJ, Jan YN, Jan LY & Cox DR (1996). Functional effects of the mouse weaver mutation on G protein-gated inwardly rectifying K$^+$ channels. *Neuron* **16**, 321–331.

Slesinger PA, Reuveny E, Jan YN & Jan LY (1995). Identification of structural elements involved in G protein gating of the GIRK1 potassium channel. *Neuron* **15**, 1145–1156.

Slesinger PA, Stoffel M, Jan YN & Jan LY (1997). Defective γ-aminobutyric acid type B receptor-activated inwardly rectifying K$^+$ currents in cerebellar granule cells isolated from weaver and Girk2 null mutant mice. *Proc Natl Acad Sci U S A* **94**, 12210–12217.

Sui JL, Petit-Jacques J & Logothetis DE (1998). Activation of the atrial KACh channel by the $\beta\gamma$ subunits of G proteins or intracellular Na$^+$ ions depends on the presence of phosphatidylinositol phosphates. *Proc Natl Acad Sci U S A* **95**, 1307–1312.

Tucker SJ & Ashcroft FM (1999). Mapping of the physical interaction between the intracellular domains of an inwardly rectifying potassium channel, Kir6.2. *J Biol Chem* **274**, 33393–33397.

Wickman KD, Iniguez-Lluhl JA, Davenport PA, Taussig R, Krapivinsky GB, Linder ME, Gilman AG & Clapham DE (1994). Recombinant G-protein $\beta\gamma$-subunits activate the muscarinic-gated atrial potassium channel. *Nature* **368**, 255–257.

Wickman K, Nemec J, Gendler SJ & Clapham DE (1998). Abnormal heart rate *regulation* in GIRK4 knockout mice. *Neuron* **20**, 103–114.

Yamada M, Inanobe A & Kurachi Y (1998). G protein *regulation* of potassium ion channels. *Pharmacol Rev* **50**, 723–757.

Yi BA, Lin Y, Jan YN & Jan LY (2001). Yeast screen for constitutively active mutant G protein-activated potassium channels. *Neuron* **29**, 657–667.

Zhang H, He C, Yan X, Mirshahi T & Logothetis DE (1999). Activation of inwardly rectifying K$^+$ channels by distinct Ptdlns(4,5)P$_2$ interactions. *Nat Cell Biol* **1**, 183–188.

Zhou W, Arrabit C, Choe S & Slesinger PA (2001). Mechanism underlying bupivacaine inhibition of G protein-gated inwardly rectifying K$^+$ channels. *Proc Natl Acad Sci U S A* **98**, 6482–6487.

Acknowledgements

Supplementary material

The online version of this paper can be found at:
    DOI: 10.1113/jphysiol.2003.056101
and contains supplementary material consisting of a figure entitled:
    Clustal alignment of rodent Kir family of channels.
    This can also be accessed at
http://www.blackwellpublishing.com
products/journals/suppmat/tjp/tjp131sm.htm